

Structure factor of diffusion-limited aggregation clusters: Local structure and non-self-similarity

C. Oh and C. M. Sorensen

Department of Physics, Kansas State University, Manhattan, Kansas 66506

(Received 6 June 1997)

The structure of diffusion-limited aggregation (DLA) clusters is studied in reciprocal (momentum) space using clusters generated by 3d cubic lattice and off-lattice simulations. Log-log plots of the structure factor $S(q)$ vs the momentum transfer q show that for DLA clusters $S(q)$ is not proportional to q^{-D} in the fractal regime, where $D \approx 2.5$ is the mass fractal dimension. A power law behavior is observed only in a limited range of large q and, moreover, the exponent is ~ -1.75 . A direct comparison with diffusion limited cluster aggregation (DLCA) clusters shows that the two structure factors are the same in the range of $q \gtrsim 0.1a^{-1}$, where a is the monomer radius. We interpret this anomalous behavior of the DLA structure factor as an indication of a DLCA-like local structure within the DLA cluster, and the length scale of the local structure is $l_c \approx 10a$. The presence of the critical length $l_c \approx 10a$ is qualitatively confirmed by real space analyses, which we find are much less sensitive to this local structure. The existence of l_c such that $R_g > l_c > a$, where R_g is the cluster radius of gyration, shows that DLA clusters are not self-similar over the entire cluster. [S1063-651X(98)06301-6]

PACS number(s): 61.10.Eq, 02.70.-c, 68.70.+w, 05.40.+j

I. INTRODUCTION

The diffusion-limited aggregation (DLA) model [1] occupies a special position in the study of aggregating systems as the first simulation model to produce an aggregate with a nontrivial fractal dimension [2] and as a canonical example of nonequilibrium growth [3]. It is also remarkable in that its simple rule of aggregation yields a complex fractal structure, the nature of which is as yet not completely understood [4]. DLA clusters are fractal in that their mass scales with overall cluster size with a power law of noninteger fractal dimension. The fractal dimension, however, is a global property, and it cannot discern internal structural details of the cluster. Soon after the invention of DLA, it was found using real space analysis that the clusters were more complex than a simple, self-similar fractal [5]. For example, DLA clusters require slightly different exponents to describe density correlations in the radial and tangential directions [6], and, therefore, they are self-affine rather than self-similar. There has been some thought that these structural subtleties were related to the finite size of the clusters analyzed, but recent work with very large clusters continues to find non-self-similarity [4]. Lack of self-similarity can imply length scales beyond overall cluster size and monomer size, but no additional length scales have as yet been found.

Despite the long history of DLA study, relatively little attention has been paid to the structure factor of DLA clusters [7–9]. In this paper we use the static structure factor to explore the structure of computer generated, three-dimensional, DLA aggregates. The structure factor resides in reciprocal space, hence our study differs significantly from previous structural studies that have reviewed DLA aggregates in real space [10–12]. We find that this reciprocal space viewpoint is very able to uncover structural properties that appear subtle with real space analysis. In particular, we find DLA clusters have a local structure that is quantitatively similar to the structure of diffusion-limited cluster aggregation (DLCA) clusters [13,14]. This structure dissolves for

length scales greater than a characteristic length of approximately ten monomer radii. This “third” length scale quantifies the manner in which the clusters are not self-similar, and it is readily apparent in the structure factor. This behavior is distinctly different from the dielectric breakdown model (DBM) [15], which is often cited as yielding structures very similar to DLA [3] but for which results available in the literature do not show this extra, characteristic length in the structure factor [9]. We also show that the overall mass fractal behavior is preserved in the structure factor by a large hump near the inverse cluster size that results from the roughly spherical, hence sharply cut off, density distribution.

In what follows we describe our simulation and structure factor results. We also study real space analysis and show faint consistency with the definite results of reciprocal space.

II. SIMULATION

We performed DLA simulations on a 3d cubic lattice and 3d off lattice adopting the algorithm introduced by Meakin [16]. For the 3d cubic lattice simulation a seed particle was initially placed at the origin. Then a monomer particle was released on a spherical shell centered at the origin with the radius r_{rel} , called the release radius, and equal to $r_{\text{far}} + 5\delta$, where r_{far} is the farthest distance between the origin and the monomers of the cluster measured in units of the lattice spacing δ . The monomer radius is $a = \delta/2$. The released particle was allowed to move randomly to one of the six nearest lattice sites with each iteration. While moving, if the particle came to occupy the nearest-neighbor site of a monomer of the cluster, it was stuck to the cluster permanently and a new particle was released. If the particle wandered off too far from the origin, the particle was killed and a new particle was released. The killing radius was $3r_{\text{far}}$. For small clusters $3r_{\text{far}}$ could be smaller than $r_{\text{far}} + 5\delta$. When this happened, a particle would be killed as soon as it was released. To correct this problem, the killing radius was set to 15δ when r_{far}

$< 5\delta$. The simulation was terminated after the desired number of iterations.

For the 3d off-lattice simulations, the killing radius and the release radius were determined in the same way. In this case, however, the diffusing particle was allowed to move in any direction (not restricted by the lattice) by a given step size. After each move, it was tested to determine whether the diffusing particle overlapped with any of the monomers of the cluster. If there was no overlap, it was allowed to diffuse again. If overlap was found, the diffusing monomer was placed where the first contact was made and the monomer was incorporated into the cluster. In the off-lattice simulations we used step size control introduced by Meakin. If the distance between the diffusing particle and the origin was less than $r_{\text{far}} + 10\delta$, the step size was δ . If the distance was larger than $r_{\text{far}} + 10\delta$, the step size was 2δ . If the distance was larger than $r_{\text{far}} + 20\delta$, the step size was 4δ , etc., continuing in a geometric fashion.

For the purpose of comparison, we also performed DLCA simulations on a 3d cubic lattice using the standard algorithm [13,14]. The details of the simulation process have been reported elsewhere [17].

III. RESULTS

A. Reciprocal space. The structure factor

The structure factor of an aggregate is defined by

$$S(\vec{q}) = \sum_{i,j} e^{i\vec{q}\cdot(\vec{r}_i - \vec{r}_j)}. \quad (1)$$

Here \vec{r}_i and \vec{r}_j are the positions of the i th and j th monomers and \vec{q} is the momentum transfer given by

$$\vec{q} = \vec{k}_s - \vec{k}_i, \quad (2)$$

where \vec{k}_i and \vec{k}_s are the wave vectors of the incident and scattered fields. For elastic scattering $k_s = k_i = 2\pi/\lambda$, hence $q = (4\pi/\lambda)\sin(\theta/2)$, where θ is the scattering angle and λ is the wavelength of the incident wave. For a self-similar fractal aggregate with a fractal dimension D , assuming a spherical symmetry, $S(\vec{q})$ has the following three regimes:

$$S(q) \propto \begin{cases} N^2 & \text{for } q < 1/R_g \\ q^{-D} & \text{for } 1/R_g < q < 1/a \\ N & \text{for } q > 1/a, \end{cases} \quad (3)$$

where R_g is the cluster radius of gyration, a is the monomer radius, and N is the number of monomers in the cluster. This behavior of $S(q)$ reflects the fact that for a truly self-similar fractal aggregate there are only two length scales. These two length scales mark the minimum and maximum distances between which the object is self-similar. For a cluster the maximum length is the cluster size represented by R_g , and the minimum length is the monomer size represented by a . A simple argument based on mass conservation [18] and the continuity of $S(q)$ at $q = 1/R_g$ shows that

$$S(q) = Nk_0(qa)^{-D} \quad (4)$$

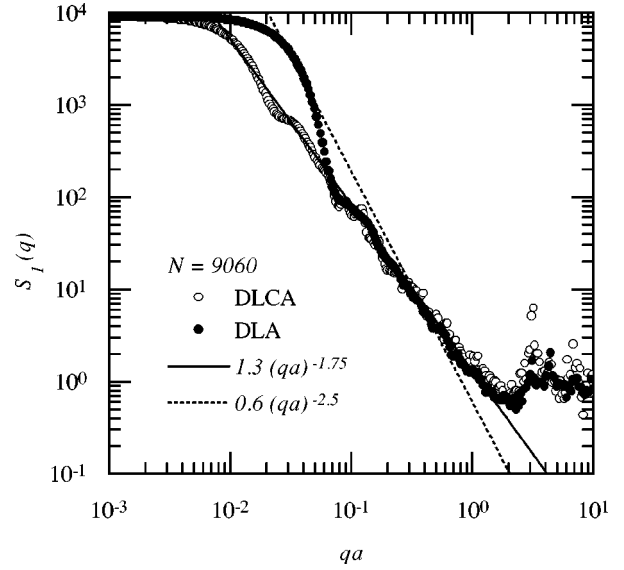


FIG. 1. A comparison of the DLA and the DLCA structure factors. Both clusters are created through simulations on a cubic lattice, and both have $N=9060$. R_g of the DLA cluster is $50.27a$.

in the fractal regime, where $1/R_g \lesssim q \lesssim 1/a$. Here k_0 is a prefactor defined in the relation

$$N = k_0 \left(\frac{R_g}{a} \right)^D \quad (5)$$

between the number of monomers and the radius of gyration. In previous work we have found $k_0 = 1.3$ for the DLCA process and $k_0 = 0.6$ for the DLA process in three dimensions [19] and it is well known that $D \approx 1.75$ and 2.5 , respectively. Even though Eqs. (3) and (4) describe the structure factor of various fractal aggregates [20–24], here we find them no longer simply applicable to DLA aggregates.

Figure 1 shows the structure factors of both DLA and DLCA clusters with the same N . Both clusters were created through simulations on a 3d cubic lattice. The structure factors shown in Fig. 1 were calculated using Eq. (1) and normalized as

$$S_1(q) = \frac{1}{N} S(q). \quad (6)$$

The solid line and the dotted line are the structure factor expected by Eq. (4) for DLCA and DLA clusters, respectively. A remarkable point about Fig. 1 is that in a linear regime extending from $q \approx 0.1a^{-1}$ to a^{-1} both structure factors are described by the DLCA version of Eq. (4). That is, they are the same, not only the slope as described by D but also the absolute value as described by the prefactor k_0 . The figure also shows that the large q ($qa > \pi$) behaviors of the two structure factors are very similar to each other, which implies that the short range monomer-monomer correlations are the same as well. Another interesting feature of the DLA structure factor in Fig. 1 is that there is a pronounced hump for $qR_g \approx 1$. This hump rises quickly with decreasing q and compensates for the -1.75 slope, which is too small to account for DLA mass fractal dimension of 2.5 . The dashed line in Fig. 1 has a slope of $-D = -2.5$ and shows that the

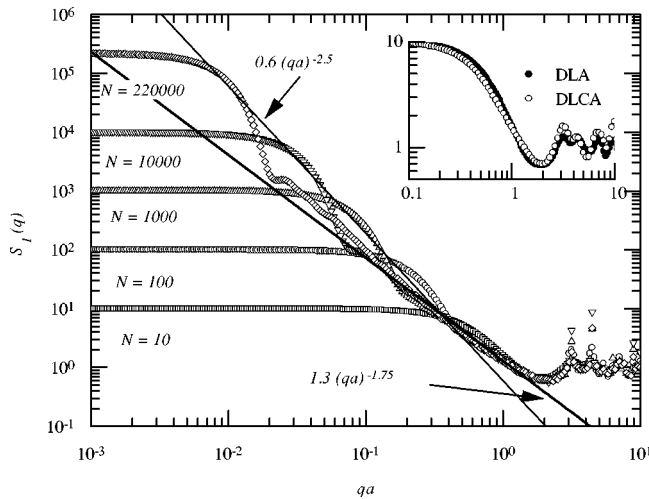


FIG. 2. The evolution of the DLA structure factor with N . The clusters are created through on-lattice simulation. The inset shows the closeup of the DLA and the DLCA structure factor for $N=10$.

hump at $q \approx R_g^{-1}$ is related to the monomer length scale at $q \approx a^{-1}$ in the manner expected by the fractal regime of Eq. (3).

The agreement between the DLCA and DLA structure factors from the intermediate to large q regime, i.e., $q \gtrsim 0.1a^{-1}$, shown in Fig. 1 means that the local environment of a DLA cluster is very similar to that of a DLCA cluster, where “local” implies length scales ranging up to $\sim 10a$. We offer two qualitative arguments why this is so by comparing the growth mechanisms of DLA and DLCA clusters. First, consider an early stage of the DLCA process when the average cluster size is small and there are still plenty of monomers left. At such a stage, the monomer-cluster collision would have a significant contribution to the cluster growth. Therefore, if one were to follow a particular cluster and watch how it grows, it would be impossible to tell whether it is a DLCA or a DLA process. Only when the cluster size is large and monomers are sufficiently depleted, would it be clear that it is not DLA.

Second, the essence of the DLA process is the addition of particles to a cluster through the diffusive motion of monomer particles. The asymptotic structure of a DLA cluster is achieved when a cluster is much greater than the diffusing particles. However, even then (and throughout the aggregation process) it is only a small section of a cluster that a particular monomer particle sees when close to a large cluster and, hence, about to join the cluster. This situation is more like the early stage of the DLCA process because the joining monomer attaches to a comparatively sized subsection of the cluster. It is the diffusive nature of the motion that determines how the monomers are arranged locally. Hence a local DLCA-like structure is obtained and preserved throughout the growth process.

The importance of the diffusive motion can be dramatically illustrated by comparing the DLA structure factor to the structure factor of a cluster created in the dielectric breakdown model (DBM) [15]. The DBM structure factor does not show any sharp hump near $q \sim R_g^{-1}$ and the slope in the $R_g^{-1} < q < a^{-1}$ regime is uniform and equal to the fractal dimension [9]. In other words, the DBM structure factor fol-

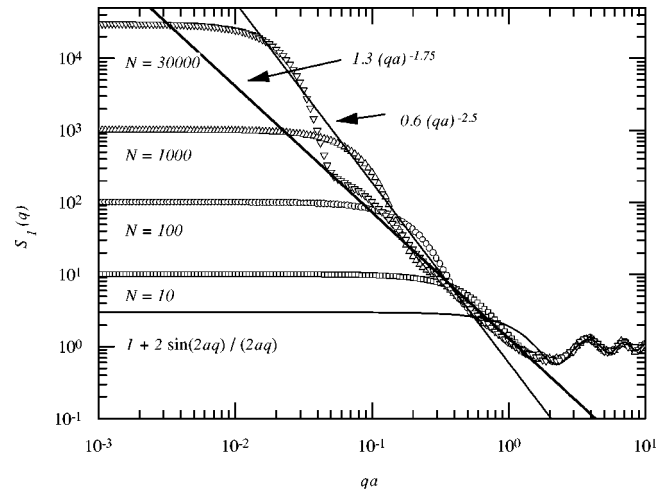


FIG. 3. The evolution of the DLA structure factor for off-lattice simulated clusters.

lows the generic pattern expected for a self-similar fractal cluster as described by Eq. (3), but the DLA structure factor does not. This abnormal behavior of the DLA structure factor does not appear to be the result of the finite size effect because the similarly sized DBM clusters do not show such a peculiar structure factor. This difference between DLA and DBM structure factors suggests that there is a generic difference between the two models even though the mean field theory shows that DBM is equivalent to DLA when the growth parameter $\eta=1$ [25]. According to the mean field consideration, the difference between the two models is in the boundary conditions for the corresponding Laplace equations. At the moment, we are not sure how the difference in the boundary conditions would translate into the structure factors. In terms of the simulations point of view, however, the difference lies in the fact that DLA is a kinetics driven model while DBM is a local instability (noise) driven model. This subtle difference may not be seen clearly in the real space analysis. Yet the difference is clearly revealed through the structure factor analysis.

We now explore the dependency of the DLCA-like structure on the overall size of the DLA cluster. In Figs. 2 and 3 we show several $S_1(q)$ for different values of N for on- and off-lattice simulations, respectively. Figure 2 is the average of five clusters and Fig. 3 is the average of ten clusters of the same size. Also shown are two straight lines, one representing the DLA-like behavior [$S_1(q) = 0.6(qa)^{-2.5}$] and the other the DLCA-like behavior [$S_1(q) = 1.3(qa)^{-1.75}$] expected from Eq. (4). Figures 2 and 3 show that the pattern of the DLA structure factor is independent of the underlying lattice structure.

For $N=10$ on a cubic lattice, the structure factor shown in Fig. 2 is indistinguishable from that of DLCA clusters of the same size. This is reasonable because for such a small cluster, the distinction between the two processes is meaningless. For $N=100$, the DLA structure factors in Figs. 2 and 3 already show a well developed hump and a linear part with the slope -1.75 . As the clusters grow further, the linear part with the slope of -1.75 is extended further to lower q until it is finally transformed into a hump at $qR_g \approx 1$. Only for the largest cluster ($N=220\,000$) is there an indication of a transitory behavior ($R_g^{-1} \lesssim q \lesssim 0.1a^{-1}$) between the linear part

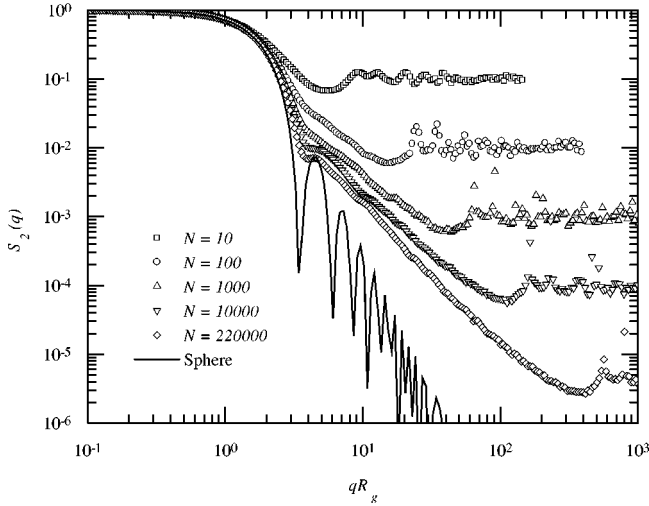


FIG. 4. A comparison of the hump in the DLA structure factor with the sphere structure factor. The sphere structure factor is calculated with the Rayleigh-Gans theory. With increasing N , the shape of the hump becomes increasingly similar to that of the sphere structure factor. The clusters are created through on-lattice simulation.

and the hump. From this we can conclude that the DLCA-like structure persists over a range of $\lesssim 10a$.

Hasmey *et al.* [24] showed that for $qa > \pi$ the general behavior of the DLCA structure factor can be explained in terms of the nearest-neighbor monomer correlation, i.e.,

$$S_1(q) \sim 1 + z \frac{\sin(2aq)}{2aq}, \quad (7)$$

where z is the number of nearest neighbors for each monomer, $z \approx 2$. Here we find that Eq. (7) also describes the structure factor of DLA clusters for the large q regime (see Fig. 3). The difference between Figs. 2 and 3 for $qa > \pi$ is caused by the different aggregation schemes, on lattice vs off lattice. Thus we conclude that DLA aggregates have a DLCA-like structure from monomer correlation up to $\sim 10a$.

The next question is, why is there a hump? Here we show that it is due to the spherical nature of DLA clusters. Figures 4 and 5 show the structure factors normalized as

$$S_2(q) = \frac{1}{N^2} S(q) \quad (8)$$

for the same DLA clusters shown in Figs. 2 and 3. Also plotted is the structure factor of a sphere calculated with the Rayleigh-Gans theory, $S(q) = [3(\sin qR - qR \cos qR)/(qR)^3]^2$, where R is the sphere radius. Note that $R_g = \sqrt{3/5}R$ for a homogeneous sphere. The figures show that for $qR_g \sim 1$, $S_2(q)$ is the same regardless of the cluster size. A comparison with the sphere structure factor shows a strong similarity between the sphere structure factor and the DLA structure factor, more so for larger clusters. This close similarity implies that the structure of the hump is strongly influenced by the spherical shape of the clusters. According to Garik [26], the shape of the DLA clusters asymptotically approaches a spherically isotropic shape. This evolution is somewhat indicated in Figs. 4 and 5. As the clusters grow, the DLA struc-

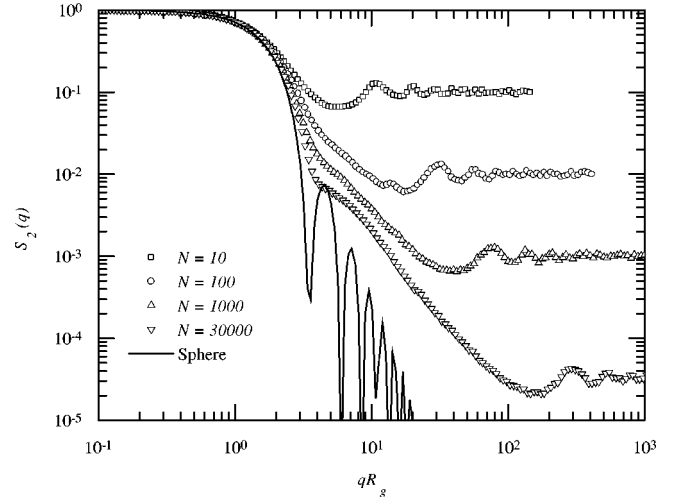


FIG. 5. The same as Fig. 4 for off-lattice simulated clusters.

ture factor follows the sphere structure factor over an increasing range of q , hence has a more spherelike character. For large clusters in Figs. 4 and 5, not only the shape of the first hump but also the positions of the second and possibly the third peaks agree well with the sphere structure factor.

We may now summarize the results above to obtain a complete description of the structure factor of a DLA aggregate. There are three length scales involved, monomer size a , an intermediate length scale $l_c \approx 10a$, and the cluster size R_g . For $q \geq l_c^{-1}$ the DLA structure factor is well described by the DLCA structure factor. This includes the monomer-monomer nearest-neighbor correlation regime $q > a^{-1}$ and the regime $l_c^{-1} \leq q \leq a^{-1}$, where the correlation between many monomers, i.e., subsections of the cluster, is quantitatively DLCA-like. For our largest clusters the region $R_g^{-1} \leq q \leq l_c^{-1}$ is ill-defined, and future work with yet larger clusters should examine this region more thoroughly. Regardless of that, near $q \approx R_g^{-1}$ a large hump appears that is the result of the overall spherical shape of the DLA cluster. Two important conclusions may then be drawn: (i) the local, i.e., length scale less than $10a$, structure of a DLA cluster is quantitatively similar to DLCA clusters, and (ii) the DLA aggregate is not self-similar over the entire range from monomer to cluster size because of the intermediate length scale l_c .

In order to further understand the local structure of DLA clusters and to confirm the existence of l_c , in the following sections we analyze DLA clusters with various methods in real space.

B. Real space

1. The two-point correlation function

The two-point correlation function $g(r)$ was calculated for the DLA clusters created through off lattice simulations. First a monomer was chosen randomly. Then the distances r between the chosen monomer and all the other monomers were calculated. The histogram $N(r, \Delta)$ of the distance distribution was obtained by counting the number of distances in the interval $(r, r + \Delta)$. The histogram was averaged for 5000 different choices of monomers. From the histogram, the two-point correlation function was readily obtained as

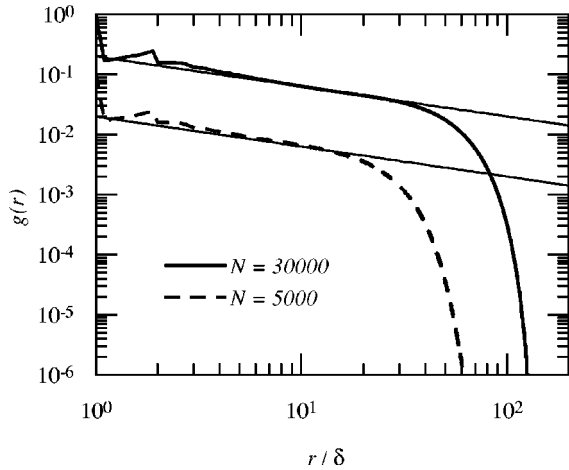


FIG. 6. Two-point correlation function of DLA clusters. The data curve for $N=5000$ is shifted downward by a decade for the clarity of the illustration. The straight lines show the expected power law behavior, r^{D-d} .

$$g(r) = \frac{N(r, \Delta)}{4\pi r^2 \Delta}. \quad (9)$$

This correlation function has been extensively studied for DLA clusters by many authors and found to be

$$g(r) \sim r^{D-d} h(r/\xi), \quad (10)$$

where d is the space dimension and $h(r/\xi)$ is the cutoff function. In many cases, however, the resolution Δ was too large (a few lattice spacing) to reveal the local structure. Moreover, the short range behavior of the correlation function of a DLA cluster has never been analyzed in conjunction with the structure factor.

Figure 6 shows $g(r)$ calculated for clusters with $N=5000$ and $30\,000$ with $\Delta=0.1\delta$. The power law behavior expected by Eq. (10) is illustrated by straight lines with a slope -0.5 . The peaks at $r/\delta=1.0$ and $r/\delta=1.98\pm 0.01$ (obtained with $\Delta=0.01\delta$) correspond to the first and second nearest monomer positions. Similar structures have been observed both in hard sphere packing [27] and DLCA [24]. From the position of the second peak we estimate the average angle between two successive bondings in a DLA cluster to be $\sim 11^\circ$.

A comparison between a straight line representing r^{D-d} and the calculated $g(r)$ shows that for $N=5000$ $g(r)$ has not fully developed the expected linear behavior indicative of a power law on a log-log plot. For $N=30\,000$, $g(r)$ shows the linear, power law behavior in the range of $5\delta \lesssim r \lesssim 30\delta$, which is only about a decade. The upper limit of the range $r \approx 30\delta$ shows a reasonable agreement with the average radius of gyration of the clusters, which we calculated to be $R_g = 38\delta$. More interesting for our work here is that the value for the lower limit $r/\delta \approx 5$ is twice as large as the value reported for DLCA clusters by Hasmey *et al.*, indicating a longer transient regime for DLA clusters. Recall that $\delta = 2a$. We believe that this transient behavior of $g(r)$ in the range $1 \lesssim r/a \lesssim 10$ is a faint, real-space realization of the

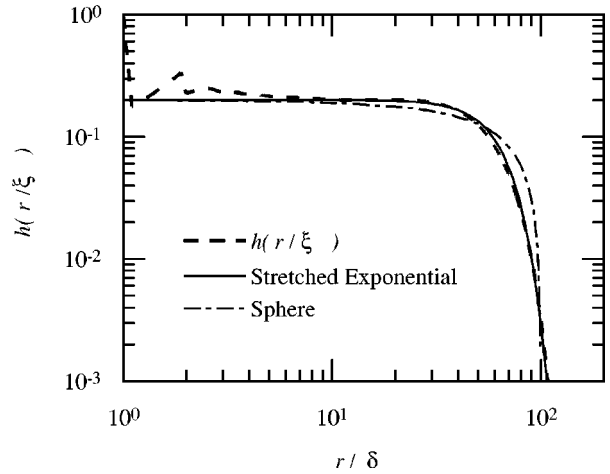


FIG. 7. The cutoff function (dashed line) for a DLA cluster with $N=30\,000$. The solid line is a fit using a stretched exponential function. The dot-dashed line is a cutoff function of a sphere with the same R_g .

short range DLCA-like structure shown more intensely in the q -space structural representations of $S(q)$ in the range $l_c^{-1} (\approx 0.1a^{-1}) \lesssim q \lesssim a^{-1}$.

In order to find the cutoff function, $g(r)r^{d-D}$ is plotted in Fig. 7 for $N=30\,000$. By fitting the data from $r/\delta=10$ to 135 to a stretched exponential function, $\sim \exp[-(r/\alpha)^\beta]$, we find $\alpha \approx 1.68R_g$ and $\beta=3.4$. A Gaussian cutoff function proved too slow to adequately fit the data, especially for large r . According to Jullien [28], a sharp cutoff function such as $\exp[-(r/\alpha)^\beta]$ with $\beta=3.4$ should lead to a hump in the structure factor for $q \sim R_g^{-1}$. In other words, the hump in the structure factor is the result of the cutoff function being so sharp. This is consistent with our conclusion that the hump results from the spherical shape of the DLA cluster because a sphere has a sharp cutoff.

2. Box counting

The clusters created by the on-lattice simulation were investigated using the box counting method instead of the two-point correlation function. The reason why we chose the box

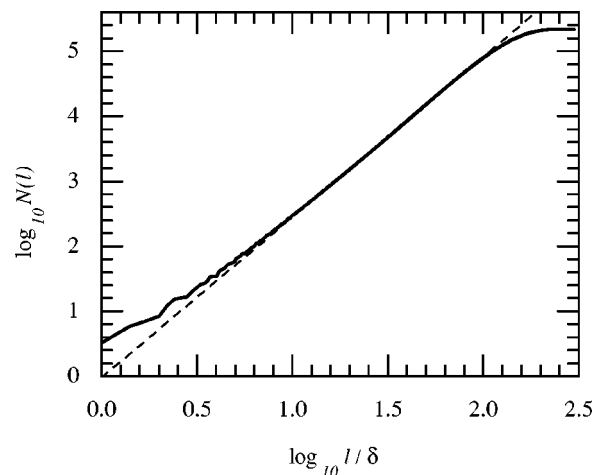


FIG. 8. $\log_{10} N(l)$ vs $\log_{10} l/\delta$ for cubic lattice simulated DLA clusters with $N=220\,000$.

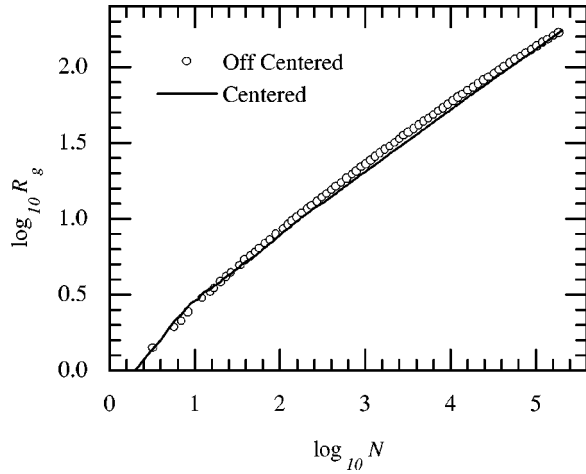


FIG. 9. A comparison of $\log R_g$ vs $\log N$ for centered and off-centered calculations. $N=220\,000$.

counting method was because the discrete nature of the lattice made it impossible to obtain a smooth $g(r)$ especially at short range.

We considered a sphere of radius l centered on an arbitrarily chosen monomer (not necessarily at the center) and counted the number of monomers in the sphere $N(l)$. The value of l was not limited to remain within the nearest edge of the cluster because we wish to compare this real space method to the reciprocal space, structure factor result which, by Eq. (1), has no restriction. The average $N(l)$ was computed by performing this procedure for 10 000 randomly chosen centers. Figure 8 shows $N(l)$ vs l averaged for five clusters with $N=220\,000$. Because the centers of our sampling spheres can lie anywhere within the cluster, this method yields the average local structure when l is small. By fitting the data from $l/\delta=10$ to 100, we found the slope to be 2.47, which is in good agreement with the fractal dimension. For $l/\delta \lesssim 10$ the plot continuously curves to a lesser slope with decreasing l , hence smaller effective fractal dimension. This, we contend, is a faint, qualitative indication of the DLCA-like structure readily apparent in q space.

3. Radius of gyration

We investigated the radius of gyration with two different approaches. First, following the traditional analysis, the radius of gyration $R_g(N)$ was calculated for given values of N as a DLA cluster grew. The other approach is similar to the box counting method above in that we considered spheres of radius l centered on randomly chosen monomers. The number of monomers within the sphere $N(l)$ was counted and the radius of gyration of the spherical section of the cluster $R_g(l)$ was calculated as a function of l . $N(l)$ and $R_g(l)$ were averaged for 10 000 different choices of the centers.

Figures 9 and 10 show the result for on- and off-lattice simulations. By fitting $\log R_g$ vs $\log N$ data in Fig. 9 to a linear function from $N=100$ to 220 000, we find a slope of 0.4036 to imply a fractal dimension $D=2.48$ as expected for a 3d

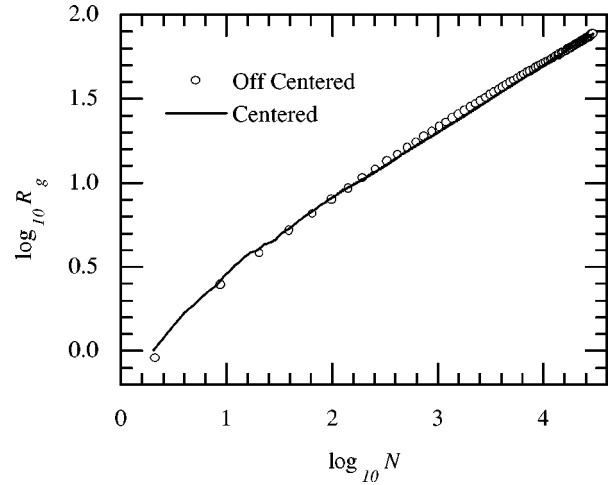


FIG. 10. The same as Fig. 9 for off-lattice simulated clusters. $N=30\,000$.

DLA aggregate. Note, however, that for both lattices and for both N vs R_g centered on the cluster and averaged over randomly chosen centers, deviations to higher slopes, hence smaller effective fractal dimension, occur for $N < 100$. Once again, these real space results faintly show that the local structure throughout the cluster has an effective fractal dimension less than the global dimension, i.e., it is more DLCA-like as quantitatively demonstrated in q space. Both Figs. 9 and 10 show more curvature for the off-centered analysis than the centered analysis. The off-centered analysis is a truer test of fractal scaling because it does not emphasize the special center point of the cluster. Thus the off-centered analysis shows that the DLA cluster is not strictly self-similar, in agreement with the structure factor analysis. Both these analyses affect an average over all points in the cluster.

IV. CONCLUSIONS

The structure factor of DLA aggregates does not show simple scaling described by q^{-D} in the range $R_g^{-1} \lesssim q \lesssim a^{-1}$, where D is the mass fractal dimension of the aggregate. Instead, a third length scale $l_c \sim 10a$ is needed to describe $S(q)$. For $q \gtrsim l_c^{-1}$ the DLA $S(q)$ is essentially identical to the DLCA $S(q)$. This result indicates that the local structure, i.e., length scales less than $10a$, of a DLA aggregate is quantitatively similar to a DLCA aggregate. The lack of simple scaling for DLA is also distinctly different from DBM structures, which are otherwise very similar to DLA. Attempts to see this local structure in real space analyses of DLA clusters were qualitatively successful but much less distinct than the reciprocal space analysis of $S(q)$. Thus the reciprocal space analysis is a powerful method to explore the structural subtleties of aggregates.

ACKNOWLEDGMENTS

This work was supported by NSF Grant Nos. CTS9408153 and CTS9709764.

- [1] T. A. Witten, Jr. and L. M. Sander, *Phys. Rev. Lett.* **47**, 1400 (1981).
- [2] B. B. Mandelbrot, *The Fractal Geometry of Nature* (Freeman, San Francisco, 1982).
- [3] T. Vicsek, *Fractal Growth Phenomena* (World Scientific, Singapore, 1992).
- [4] B. B. Mandelbrot, A. Vespignani, and H. Kaufman, *Europhys. Lett.* **32**, 199 (1995).
- [5] P. Meakin, in *Phase Transitions and Critical Phenomena*, edited by C. Domb and J. L. Lebowitz (Academic Press, New York, 1987), Vol. 12, p. 335.
- [6] P. Meakin and T. Vicsek, *Phys. Rev. A* **32**, 685 (1985).
- [7] P. W. Schmidt, G. Pipitone, M. A. Floriano, E. Caponetti, and R. Triolo, in *Materials Research Society Symposium Proceedings*, edited by F. Family, P. Meakin, B. Sapoval, and R. Wool (Materials Research Society, Pittsburgh, 1996), Vol. 367, p. 429.
- [8] J. G. Amar and F. Family, *Phys. Rev. B* **50**, 8781 (1994).
- [9] A. Pearson and R. W. Anderson, *Phys. Rev. B* **48**, 5865 (1993).
- [10] J. Vannimenus and X. G. Viennot, *J. Stat. Phys.* **54**, 1529 (1989).
- [11] E. L. Hinrichsen, K. J. Maloy, J. Feder, and T. Jossang, *J. Phys. A* **22**, L271 (1989).
- [12] P. Ossadnik, *Phys. Rev. A* **45**, 1058 (1992).
- [13] P. Meakin, *Phys. Rev. Lett.* **51**, 1119 (1983).
- [14] M. Kolb, R. Botet, and R. Jullien, *Phys. Rev. Lett.* **51**, 1123 (1983).
- [15] L. Niemeyer, L. Pietronero, and H. J. Wiesmann, *Phys. Rev. Lett.* **52**, 1033 (1984).
- [16] P. Meakin, *Phys. Rev. A* **27**, 1495 (1983).
- [17] C. Oh and C. M. Sorensen, *J. Colloid Interface Sci.* **193**, 17 (1997).
- [18] T. A. Witten and L. M. Sander, *Phys. Rev. B* **27**, 5686 (1983).
- [19] C. M. Sorensen and G. C. Roberts, *J. Colloid Interface Sci.* **186**, 447 (1997).
- [20] H. D. Bale and P. W. Schmidt, *Phys. Rev. Lett.* **53**, 596 (1984).
- [21] P. Dimon, S. K. Sinha, D. A. Weitz, C. R. Safinya, G. S. Smith, W. A. Varady, and H. M. Lindsay, *Phys. Rev. Lett.* **57**, 595 (1986).
- [22] X. Wen, C. W. Garland, T. Hwa, M. Kardar, E. Kokufuta, Y. Li, M. Orkisz, and T. Tanaka, *Nature (London)* **355**, 426 (1992).
- [23] T. Freltoft, J. K. Kjems, and S. K. Sinha, *Phys. Rev. B* **33**, 269 (1986).
- [24] A. Hasmy, M. Foret, J. Pelous, and R. Jullien, *Phys. Rev. B* **48**, 9345 (1993).
- [25] L. Pietronero and H. J. Wiesmann, *J. Stat. Phys.* **36**, 909 (1984).
- [26] P. Garik, *Phys. Rev. A* **32**, 1275 (1985).
- [27] C. H. Bennett, *J. Appl. Phys.* **43**, 2727 (1972).
- [28] R. Jullien, *J. Phys. I* **2**, 759 (1992).